EUROPEAN ORGANIZATION FOR NUCLEAR RESEARCH

CERN–PPE/93–63
31 March 1993

Measurement of the reaction $\bar{p}p \to K_S K_S$ in the region near $\sqrt{s} \approx 2230$ MeV

P.D. Barnes[1,a], P. Birien[3], W.H. Breunlich[7], G. Diebold[1,b], W. Dutty[3], R.A. Eisenstein[4], G. Ericsson[6], W. Eyrich[2], H. Fischer[3], R. von Frankenberg[2], G. Franklin[1], J. Franz[3], R. Geyer[2,c], N. Hamann[3,d], D. Hertzog[4], P. Hoffmann[3], A. Hofmann[2,†], T. Johansson[6], K. Kilian[5], R.-A. Kraft[2], C. Maher[1], N. Nägele[7], W. Oelert[5], S. Ohlsson[6,e], B. Quinn[1], E. Rössle[3], H. Schledermann[3], H. Schmitt[3], G. Sehl[5], J. Seydoux[1], F. Stinzing[2], R. Todenhagen[3] and H.-J. Urban[3]

1) Carnegie–Mellon University, Pittsburgh, PA 15213, USA
2) University of Erlangen–Nürnberg, D–8520 Erlangen, Germany
3) University of Freiburg, D–7800 Freiburg, Germany
4) University of Illinois at Urbana–Champaign, Urbana, IL 61801, USA
5) Institut für Kernphysik der KFA, D–5170 Jülich, Germany
6) Uppsala University, S–75121 Uppsala, Sweden
7) Institut für Mittelenergiephysik der ÖAW, A–1090 Vienna, Austria

ABSTRACT

Measurements of the total and differential cross-sections of the reaction $\bar{p}p \to K_S K_S$ are presented for values of $\sqrt{s}$ in the region near 2230 MeV. The 18 energies of the scan were chosen to permit a sensitive search for resonant structure related to the $\xi(2230)$ state in a channel with a minimal non-resonant background. No such structure is observed. Stringent limits for the branching ratio are set based on various assumptions for the width and spin of the ξ.

(Submitted to Physics Letters B)

---

† Deceased.

a) Present address: LAMPF, Los Alamos, NM 87545, USA.

b) Present address: Yale University, New Haven, CT 06511, USA.

c) Present address: Institut für Mittelenergiephysik der ÖAW, A–1090 Vienna, Austria.

d) Present address: CERN, PPE Division, CH–1211 Geneva, Switzerland.

e) Present address: IN2P3, Centre de Calcul, F–69622 Villeurbanne, France.

1. INTRODUCTION

The MARK III Collaboration [1] at SLAC–SPEAR presented evidence for a narrow state, called [2] the $\xi(2230)$, observed in the radiative decays of the $J/\psi(1S)$ to K^+K^- and K_SK_S final states. The measured parameters of this resonance, obtained after averaging the charged and neutral decay-mode results, are its mass $m_\xi = (2231 \pm 7 \pm 11)$ MeV and width $\Gamma_\xi = (22 \pm 19 \pm 14)$ MeV, where the first error is statistical and the second one is systematic. The ratio of branching fractions to the K^+K^- and K_SK_S final states, $r = 1.3 \pm 0.8 \pm 0.4$, is found to be consistent with the value 2 expected for an isoscalar resonance. The allowed quantum numbers for the ξ must lie in the series $J^{PC} = 0^{++}, 2^{++}, 4^{++}, \ldots$, since the K_SK_S decay mode is observed.

The non-observation of the ξ by the DM2 Collaboration [3] at Orsay–DCI seems to be in disagreement with the MARK III results. However, this is not too disturbing, because the results from the two J/ψ experiments are in fact consistent with each other, if the width or the branching ratio of the ξ is assumed not at the MARK III central value but just one standard deviation (1 *SD*) above or below it, respectively.

The narrow width of the ξ and the strange-quark content in the observed decays has stimulated a large number of interpretations and speculations. The resonance could be a light Higgs boson in *non*-minimal models [4], a bound state of two heavy coloured scalars [5], a glueball [6], a $\bar{q}qg$ hybrid [7,8], an ordinary $\bar{s}s$ quarkonium state in a $^3F_2$ or $^3F_4$ configuration [9], a baryonium state such as $(qs)_3(\bar{q}\bar{s})_3$ with q being a u- or d-quark [8], or an $\bar{s}s\bar{s}s$ multi-quark state [10]. Since the reported ξ mass is nearly twice the Λ mass, bound $\bar{\Lambda}\Lambda$ states [11] or threshold cusp effects [12] may be considered as well. The observation and also the *non*-observation of the ξ in different reaction channels can limit the list above, as would any additional angular momentum constraint or increased precision on the knowledge of the width.

A significant branching ratio of about 1 % for the decay of the ξ to $\bar{p}p$ is expected in some, but not all, of the models alluded to above. Therefore one may attempt to look for the ξ formation and decay by means of $\bar{p}p \to \xi \to \bar{K}K$, where the initial $\bar{p}p$ system is bound to annihilate from the spin-triplet state due to parity and charge-conjugation invariance. Experiments E789 [13] at BNL–AGS and PS170 [14] at CERN–LEAR examined the region around the reported ξ mass by measuring the ratio of cross-sections, $R = \sigma(\bar{p}p \to K^+K^-)/\sigma(\bar{p}p \to \pi^+\pi^-)$. No structure was found in the energy dependence of R. The centre-of-mass angular range accepted by these two experiments was $|\cos\theta^*| < 0.5$ and $|\cos\theta^*| < 0.77$,

respectively. The LEAR experiment PS172 [15] measured $\bar{p}p$ annihilations into K^+K^- and $\pi^+\pi^-$ final states over the full centre-of-mass angular range and found no narrow structure that could be associated with the ξ. In this case, the ratio of cross-sections R revealed a significant variation with the incident antiproton momentum, and so did some Legendre polynomial coefficients obtained from fits of angular distributions. However, any experimental result extracted for R can be interpreted as an upper limit for the product branching ratio, $BR(\xi \to \bar{p}p) \cdot BR(\xi \to K^+K^-)$, provided one assumes a certain width and spin for the ξ *and* an only negligible coupling of the ξ to $\pi^+\pi^-$.

The $\bar{p}p \to K^+K^-$ experiments suffer from the large non-resonant cross-section of about 50 μb for that channel [16]. This restricts the sensitivity of the search to relatively strong couplings of the ξ to $\bar{p}p$. In contrast, the poorly known $\bar{p}p \to K_SK_S$ channel appears to have a non-resonant cross-section that is 10 to 20 times smaller [16]. This permits a much more sensitive search for any resonance having been excited through the $\bar{p}p$ reaction and forms the basic motivation for the work reported in this paper.

Here we present the results from a scan in small bins of $\sqrt{s}$ of the total cross-section for the reaction $\bar{p}p \to K_SK_S$ in the region of the reported ξ mass. Our results set upper limits on the ξ production, which are much more stringent than those obtained in previous $\bar{p}p$ formation experiments. In addition, differential cross-section measurements for $\bar{p}p \to K_SK_S$ are reported for the first time.

2. EXPERIMENTAL DETAILS

The measurement was performed as part of the PS185 experimental programme at the CERN Low-Energy Antiproton Ring (LEAR). The apparatus was originally designed to study the reaction $\bar{p}p \to \bar{\Lambda}\Lambda$ near threshold [17]. Modifications and extensions were introduced so as to increase the acceptance for the similar $2V^0$-type reaction involving two $K_S \to \pi^+\pi^-$ decays. Unlike the $\bar{\Lambda}\Lambda$ channel in the threshold region, where the hyperons are constrained to a narrow forward cone centred around the beam axis, the K_S can be produced at any laboratory angle. Its decay length at the momenta relevant here (0.5 to 2.0 GeV/c) ranged from 3 to 10 cm over the full angular range. The apparatus used for the $\bar{p}p \to K_SK_S$ measurements is shown in Figure 1.

The antiproton beam extracted from LEAR had an average intensity of (3 to 4)·10^5 s^{-1} in a cross-sectional area of less than 1 mm^2 (FWHM). It was focused onto a segmented target system consisting of two 2.5 mm and two

5.0 mm long cylinders of polyethylene (CH_2), and one 2.5 mm long carbon cell used for background checks. Each of these target cells (see magnified view in Figure 1) was sandwiched between and surrounded by scintillation veto counters. Such a modular structure allows for a very fine localisation of any neutral interaction, which results in an improved vertex reconstruction. The momentum uncertainty of the incident beam was $\Delta p = \pm 0.3$ MeV/c at $p = 1440$ MeV/c. This figure, combined with the average momentum spread due to straggling in the cells, leads to an uncertainty $\Delta(\sqrt{s}) = \pm 0.2$ MeV for a 2.5 mm long CH_2 cell.

Two drift-chamber stacks, containing a total of 19 planes in four orientations transverse to the beam direction, were positioned downstream of the target system and served as the main decay volume for the neutral kaons (see Figure 1). Three coaxial "boxes", their sides being made of limited-streamer tubes [18] with two-dimensional digital readout, were positioned around the target system in order to record the tracks of backward-going charged pions from K_S decays.

A 44-element scintillation hodoscope was placed downstream of the drift chambers to detect the presence of charged particles about 35 cm away from the target. This information, together with a veto from the target scintillator system and with two beam-defining counters, was used in the on-line trigger in order to indicate the presence of an event type "charged–neutral–charged" characteristic for the delayed decays sought. Additional details of the detector can be found in Ref. [19].

The data were obtained at 18 incident antiproton momenta in the range from 1300 to 1570 MeV/c. The LEAR accelerator was tuned to eleven different momentum settings and a 1.5 cm long degrader (CH_2), corresponding to a 4.2 MeV/c reduction of the incident momentum, was used in combination with seven of these settings to cover the scanning region in $\sqrt{s}$. Care was taken to ensure a "continuous" scan in the region nearest to the reported ξ mass. In total, $1.52 \cdot 10^{11}$ antiprotons were incident on the target. The antiproton momenta and average values of $\sqrt{s}$ for the centre of the target system are listed in Table 1.

3. ANALYSIS

The data have been analysed in a manner similar to our previous work [17] with $2V^0$-type events. The main logical steps are briefly described here.

Establishing candidate $2V^0$ events. The first step in the data reduction requires that at least one well-measured V^0 be located inside the forward drift-chamber stack. Monte Carlo studies showed that this condition is always fulfilled for the $\bar{p}p \to K_S K_S$ events in our experiment. We define a V^0 as a pair of three-dimensional tracks having a "distance of closest approach" not larger than 3 *SD*, where the standard deviation is determined event by event from the precision with which individual tracks are measured. Next, a $2V^0$ condition is imposed, in which the two charged tracks belonging to the other V^0 may be located in any part of the detector (forward drift chambers, backward streamer tubes, or shared between both). Owing to two-body kinematics of the $\bar{p}p \to K_S K_S$ events sought, simple tests are applied. The plane spanned by each of the two decay V^0's must have a shortest "distance plane-to-target" not larger than 5 *SD* (coplanarity condition). The hypothetical straight line connecting the two vertices must pass the antiproton beam axis within 3 *SD* (collinearity condition), where the standard deviation depends on the decay distance of the V^0 particles.

Kinematic fitting. The candidate $2V^0$ events having survived the above steps are characterised by a complete set of measured "vertex parameters". They are subjected to a "kinematic fitting" procedure under the hypothesis of $\bar{p}p \to K_S K_S \to \pi^+\pi^-\pi^+\pi^-$, where the beam momentum is kept at its nominal value. A least-squares method is employed in order to determine the "kinematical parameters" of the event with improved accuracy. For a clean separation of "good events" from "background", an appropriate cut in $\chi^2_{red} \leq 5.5$ is applied. After the kinematic fitting, several procedures are used in order to obtain absolute normalisations of the data and the correct shape of cross-sections.

Beam normalisation. For each beam momentum and target cell, the integrated luminosity is determined from the number of antiprotons incident on that cell and from the data-acquisition live-time.

Acceptance correction. In the case of $\bar{p}p \to \bar{\Lambda}\Lambda$ threshold studies, the PS185 experiment has an overall acceptance that is almost 4π. Contrasting this, the $\bar{p}p \to K_S K_S$ acceptance in the centre-of-mass angular range varies between 5 and 20 %, its average value being about 10 % of 4π. This is largely due to a gap in the tracking near $\theta^{lab} \approx 80°$, as well as lower precision and efficiency of tracking in the range $95° \leq \theta^{lab} \leq 140°$ where the streamer-tube planes resided. We also take into account the fact that $K_S \to \pi^+\pi^-$ decays could send a pion in the direction of the light-guides to the target veto counters, thereby eventually producing a Cherenkov signal which would veto an otherwise good event. A Monte Carlo program has been developed to correct the measured data as a function of $\cos\theta^*$

of an emitted K_S. This correction function shows no significant dependence on $\sqrt{s}$ over the relevant energy range.

Carbon correction. For the correct normalisation of the data, the number of K_SK_S events produced from the carbon content in the CH_2 target cells must be determined. Data stemming from the special carbon target cell are therefore processed with the same analysis as those from the CH_2 cells. This revealed that the carbon contribution in our data amounts to 13.9 % when averaged over all four CH_2 target cells.

"Neutral-background" subtraction. One background channel surviving the kinematic fitting is $\bar{p}p \rightarrow K_SK_S\pi^0$. A fraction of these events remain in the fitted data sample if the energy carried away by the π^0 is small. The influence of the accompanying π^0 is to lower the effective energy of the kaons and, accordingly, to increase the angle between their decay pions. In these events, the actual hits that define the tracks fall systematically to the outside of the projected paths of the outgoing charged pions *after* kinematic fitting. Events of this type have been carefully simulated with Monte Carlo techniques. A filter has been developed and used in the data analysis to reject events with these systematic characteristics. After applying the filter, a 10.8 % contamination due to $K_SK_S\pi^0$ events is determined from measured and simulated "missing mass" spectra. For the reaction $\bar{p}p \rightarrow K_SK_S+X$, the "missing mass" is defined as $m_X^2(K_SK_SX) = E_X^2 - p_X^2$. The resulting spectrum in Figure 2 exhibits a large peak around $m_X^2 = 0$ corresponding to K_SK_S events. The contribution near $m_X^2 \approx 0.02\,\mathrm{GeV}^2$ can be attributed to the remaining intensity of contaminant $K_SK_S\pi^0$ events. The line is from a Monte Carlo simulation whose input intensity of K_SK_S and $K_SK_S\pi^0$ events reflects the cross-section ratio, $R = \sigma(\bar{p}p \rightarrow K_SK_S)/\sigma(\bar{p}p \rightarrow K_SK_S\pi^0) = 0.19 \pm 0.04$, which is consistent with previous experiments [16].

"Charged-background" subtraction. Another background channel requiring careful inspection is due to events where, in addition to four tracks satisfying the $2V^0$ condition with K_SK_S kinematics, a fifth clean track is seen in the detector. Such events can stem from quasi-free $\bar{p}n$ interactions in carbon nuclei, or from $\bar{p}p$ reactions producing a sixth track that lies outside the detection volume. Either case must be attributed to a non-zero inefficiency of the trigger veto on prompt charged particles, a subsequent unprecise reconstruction of some corresponding events, or the erroneous selection of particular vertex combinations. In two-dimensional "missing mass" spectra, $m_{X_1}^2(K_{S_1}X)$ versus $m_{X_2}^2(K_{S_2}X)$, the genuine $\bar{p}p \rightarrow K_SK_S$ events fall near $m_{X_1}^2 \approx 0.25\,\mathrm{GeV}^2 \approx m_{X_2}^2$. Essentially all background remaining in these plots has $m_X^2 \geq 1.5\,\mathrm{GeV}^2$ and is therefore easily separated [19].

After kinematic fitting and the application of the described procedures for background rejection, the number of $\bar{p}p \to K_S K_S$ events remaining in the final fitted data sample is 901. It is worth noting that this represents a 10-fold increase of the world statistics over that prior to our experiment [16].

4. RESULTS

The $\bar{p}p \to K_S K_S$ total cross-section measurements for the 18 momentum settings are displayed in Figure 3 and listed numerically in Table 1. The errors given include the statistical uncertainties of the measured event sample, as well as the errors due to carbon subtraction, acceptance correction, normalisation and background subtraction. Each entry shown corresponds to the sum taken over all four CH_2 target cells. No resonant structure is observed in the data. The weighted average of the cross-section in this energy interval is determined to be $\sigma = (1.95 \pm 0.11)$ μb.

Our data allow to quantify the possible existence of a structure on top of a non-resonant cross-section. For the latter, a parameterisation of the $\bar{p}p$ two-meson annihilation cross-section has been chosen following Ref. [20],

$$\sigma_{non-res}(E) = C q^* \exp(-2Aq^*) \tag{1}$$

with $E = \sqrt{s}$, $A = 1.2\ (\mathrm{GeV}/c)^{-1}$, and q^* denoting the K_S momentum in the centre-of-mass frame. Assuming no resonance, a fit of our data using Eqn. (1) yielded $C = (21.5 \pm 1.2)$ μb·$(\mathrm{GeV}/c)^{-1}$ which is consistent with the cross-section average as given above. The functional form

$$\sigma_{res}(E) = \frac{\pi(\hbar c)^2(2J+1)}{s-4m_p^2} \frac{\Gamma^2}{\left(E-E_{res}\right)^2 + \Gamma^2/4} BR(\xi \to \bar{p}p) \cdot BR(\xi \to K_S K_S) \tag{2}$$

describes a Breit–Wigner resonance with width Γ, mass $m = E_{res}$ and angular momentum J. A series of least-squares fits was made using Eqns. (1,2) together, with fixed inputs for Γ, E_{res} and J, in order to set 3 *SD* upper limits on the product branching ratio, $w_i \cdot w_f = BR(\xi \to \bar{p}p) \cdot BR(\xi \to K_S K_S)$. In Table 2 the results are given for two different mass values (the respective averages from Refs. [1,2]) and angular momentum $J = 4$ (the values corresponding to $J = 2$ and $J = 0$ are obtained by multiplying our numbers with factors 9/5 or 9, respectively). In all these fits, the parameter C determining the background varied only within its error.

Over the range of widths (from 1 to 30 MeV), the upper limit of the product branching ratio to the K_SK_S final state for $J = 4$ is approximately (13 to 2)·10^{-5}. An isoscalar state with quantum numbers J^{PC} = (even)$^{++}$ would decay to final states K^+K^-, K_SK_S and K_LK_L in the ratio 2:1:1. Therefore, our limits for $J = 4$ are to be compared with the results in Refs. [13,14] for $J = 2$. From these two $\bar{p}p \to K^+K^-$ experiments, the product branching ratio of a $J = 2$ resonance is given 3 *SD* upper limits of (77 to 13)·10^{-5} over a similar range of assumed resonance widths. Thus our $\bar{p}p \to K_SK_S$ experiment reported here is more sensitive at least by a factor 5.

We have found very similar K_SK_S angular distributions at all beam momenta. This is consistent with the fact that the total cross-section data of Figure 3 appear to have no significant energy dependence. Therefore, we obtained the $\bar{p}p \to K_SK_S$ differential cross-sections by grouping together all energy settings of the scan. The results are shown in Figure 4, where the errors are as detailed above. A series of fits was made using an expansion of even Legendre polynomials,

$$\frac{d\sigma}{d\Omega}(\cos\theta^*) = \sum_{k\ even}^{k_{max}} A_k P_k(\cos\theta^*). \qquad (3)$$

It turned out that only the A_0 and A_2 terms were required to fit the data. The Legendre coefficients and χ^2_{red} values obtained in the fits are given in Table 3. Our data reveal an enhancement in the forward/backward direction with respect to the central region. However, this anisotropy is much less pronounced than that predicted [21] in a baryon-exchange model with or without intermediate resonances. Finally, we note that our data presented in this paper constitute the first reported measurement of the $\bar{p}p \to K_SK_S$ differential cross-section.

5. CONCLUSIONS

We have measured at LEAR the reaction $\bar{p}p \to K_SK_S$ in the region of the reported ξ mass, $\sqrt{s} \approx 2230$ MeV. Assuming the branching ratio to all kaon pairs, $BR(\xi \to \bar{K}K)$, to be 10 % or more (a conservative estimate), our experiment reveals that the branching ratio $BR(\xi \to \bar{p}p)$ is less than 0.1 %.

Besides the original MARK III data [1] on decays $J/\psi \to \gamma\bar{K}K$, some positive experimental evidence has been forthcoming which may be interpreted [2] as the ξ. The GAMS Collaboration [22], in a joint CERN/IHEP

experiment, observed a narrow structure near 2220 MeV in the $\eta\eta'$ invariant mass spectra obtained with the reaction $\pi^-p \to \eta\eta'n$. From angular distributions of this isoscalar state it was concluded that its spin is $J \geq 2$. Experiment E147 [23] at Serpukhov measured the reaction $\pi^-p \to K_SK_Sn$. The amplitude analysis of the K_SK_S invariant mass spectrum indicated a pronounced D-wave near 2230 MeV, hence $J^{PC} = 2^{++}$. The LASS Collaboration [24] at SLAC reported results from studies of $K^-p \to \bar{K}K\Lambda$, where a structure near 2210 MeV was seen both in the K^+K^- and K_SK_S invariant mass spectra. Amplitude analyses revealed $J \geq 2$ for this state, with $J^{PC} = 4^{++}$ found to be the most likely possibility. Taken together, these informations and the results from our experiment appear to be consistent with the more traditional interpretation of the ξ as an $\bar{s}s$ meson in a $^3F_4$ configuration, or a four-quark state with significant strange-quark content, or a bound $\bar{\Lambda}\Lambda$ state.

Clearly, the ξ/f_4 awaits further experimental confirmation [2].

ACKNOWLEDGEMENTS

The measurement presented here would not have been possible without the efforts of the staff of the CERN antiproton complex, and especially of the LEAR team, in preparing the high-quality antiproton beams at numerous momentum settings. We wish to thank them for their excellent and essential contribution to our experiment.

This work is based on parts of two Doctoral Theses and one Diploma Thesis submitted by three of us (H. Schledermann, J. Seydoux and P. Hoffmann) to our respective Universities.

We gratefully acknowledge support from the Austrian Science Foundation, the CERN Experimental Physics Division, the German Federal Minister for Research and Technology (under contracts 0234 FR AI and 0234 ER A), the Swedish Natural Science Research Council, the United States Department of Energy, and the United States National Science Foundation.

REFERENCES

[1] R.M. Baltrusaitis et al., Phys. Rev. Lett. 56 (1986) 107.

[2] The state ξ is now called $f_4(2220)$ in the Review of Particle Properties, Phys. Rev. D45 (1992).

[3] J.E. Augustin et al., Phys. Rev. Lett. 60 (1988) 2238.

[4] H.E. Haber and G.L. Kane, Phys. Lett. 135 (1984) 196.
R.S. Willey, Phys. Rev. Lett. 52 (1984) 585.
R.M. Barnett et al., Phys. Lett. B136 (1984) 191.

[5] M.P. Shatz, Phys. Lett. B138 (1984) 209.

[6] B.F.L. Ward, Phys. Rev. D31 (1985) 2849.

[7] M.S. Chanowitz and S.R. Sharpe, Phys. Lett. B132 (1983) 413.
A. Le Yaouanc et al., Z. Phys. C28 (1985) 309.

[8] K.-T. Chao, Phys. Rev. Lett. 60 (1988) 2579.

[9] S. Godfrey, R. Kokoski and N. Isgur, Phys. Lett. B141 (1984) 439.

[10] S. Pakvasa, M. Suzuki and S.F. Tuan, Phys. Lett. B145 (1984) 135.

[11] S. Ono, Phys. Rev. D35 (1987) 944.

[12] K. Kilian, Proc. 5th European Symposium on Nucleon–Antinucleon Interactions, Bressanone, 1980 (CLEUP, Padova, 1980) p. 681.

[13] J. Sculli et al., Phys. Rev. Lett. 58 (1987) 1715.

[14] G. Bardin et al., Phys. Lett. B195 (1987) 292.

[15] A. Hasan et al., Nucl. Phys. B378 (1992) 3.

[16] Compilation of Cross-Sections III, report CERN–HERA/84–01 (1984).

[17] P.D. Barnes et al, Nucl. Phys. A526 (1991) 575.
P.D. Barnes et al, Phys. Lett. B189 (1987) 249.

[18] These tubes were built by us following a design by the CHARM II Collaboration: J.P. DeWulf et al., Nucl. Instr. and Meth. A252 (1986) 443.

[19] Details of the detector and analysis can be found in the Doctoral Theses of H. Schledermann (University of Freiburg, 1989) and J. Seydoux (Carnegie–Mellon University, 1990), and in the Diploma Thesis of P. Hoffmann (University of Freiburg, 1992).

[20] J. Vandermeulen, Z. Phys. C37 (1988) 563.

[21] V. Girija and F. Tabakin, Phys. Rev. C34 (1986) 1798.

[22] D. Alde et al., Phys. Lett. B177 (1986) 120.

[23] B.V. Bolonkin et al., Nucl. Phys. B309 (1988) 426.
B.V. Bolonkin et al., Sov. J. Nucl. Phys. 46 (1987) 451.

[24] D. Aston et al., Phys. Lett. B215 (1988) 199.
D. Aston et al., Nucl. Phys. B301 (1988) 525.

TABLES

Table 1. Measurement conditions and results of the scan. Momentum values and centre-of-mass energies are given for the centre of the target system. For each incident momentum, the integrated luminosity and the total cross-section value correspond to the sum of results from the four individual target cells.

$\bar{p}$ momentum [MeV/c]	$\sqrt{s}$ [MeV]	$\int L\,dt$ [μb^{-1}]	$\sigma(\bar{p}p \to K_S K_S)$ [μb]
1297.1	2182.9	647.22	2.34 ± 0.51
1361.8	2205.5	591.54	2.43 ± 0.58
1366.0	2206.9	767.94	2.41 ± 0.49
1400.8	2219.1	654.36	1.87 ± 0.48
1405.0	2220.6	761.70	2.63 ± 0.54
1418.2	2225.3	610.50	1.86 ± 0.49
1422.4	2226.7	699.18	2.08 ± 0.48
1428.1	2228.7	617.64	1.53 ± 0.41
1432.3	2230.2	798.90	2.04 ± 0.46
1437.1	2231.9	585.00	1.99 ± 0.51
1441.3	2233.4	798.00	1.76 ± 0.41
1445.8	2235.0	401.94	2.08 ± 0.59
1450.0	2236.4	670.86	1.46 ± 0.41
1464.8	2241.7	770.46	1.90 ± 0.44
1469.0	2243.1	665.40	1.63 ± 0.41
1487.4	2249.6	935.76	2.16 ± 0.43
1503.9	2255.4	600.18	1.55 ± 0.44
1564.9	2277.0	1090.08	2.23 ± 0.41

Table 2. Results from fits of the total cross-section data to a background plus a Breit–Wigner resonance using Eqns. (1,2) together. For a variety of resonance parameters, $m = E_{res}$ and Γ, upper limits corresponding to 3 *SD* are given for the product branching ratio, $w_i \cdot w_f = BR(\xi \to \bar{p}p) \cdot BR(\xi \to K_S K_S)$. The value $J = 4$ has been assumed, however, limits for $J = 2$ and $J = 0$ can be obtained by multiplying the $w_i \cdot w_f$ columns with factors 9/5 or 9, respectively.

Γ	m = 2231 MeV		m = 2225 MeV	
[MeV]	$w_i \cdot w_f$ [$\cdot 10^{-5}$]	$\sigma_{res}(E_{res})$ [μb]	$w_i \cdot w_f$ [$\cdot 10^{-5}$]	$\sigma_{res}(E_{res})$ [μb]
1	12.68	3.83	6.45	1.99
3	4.02	1.22	4.41	1.36
10	2.15	0.65	2.59	0.80
30	1.51	0.46	1.61	0.50

Table 3. Results from fits of the differential cross-section data to even Legendre polynomial expansions using Eqn. (3). For the cross-sections all momentum settings of the scan have been grouped together. The three rows show coefficients and χ^2_{red} values which have been obtained including polynomials up to order 0, 2 or 4, respectively. For $k_{max} \geq 2$, the implied integrated cross-section, $\sigma = 2\pi A_0$ [μb], is consistent with the weighted average given in section 4.

$\bar{p}$ momenta [MeV/c]	$\sqrt{s}$ range [MeV]	A_0	A_2	A_4	χ^2_{red}
1297 – 1565	2183 – 2277	0.261 ± 0.013	—	—	3.62
1297 – 1565	2183 – 2277	0.300 ± 0.014	0.224 ± 0.032	—	1.05
1297 – 1565	2183 – 2277	0.306 ± 0.015	0.190 ± 0.036	-0.107 ± 0.051	0.85

FIGURE CAPTIONS

Figure 1. Layout of the PS185 detector arrangement with: (1) trigger-active target system, see magnified view; (2) 13-plane drift chamber stack; (3) 6-plane drift chamber stack; (4) scintillator hodoscope; (5) solenoidal magnet (0.1 T) including three drift-chamber planes; (6) concentric arrays of limited-streamer tubes. A typical event $\bar{p}p \to K_S K_S \to \pi^+\pi^-\pi^+\pi^-$ is superposed. Note that the magnet information is not used in this particular experiment.

Figure 2. Spectrum of the "missing mass", $m_X^2(K_S K_S X)$, after kinematic fitting and after applying the "neutral-background" filter discussed in the text. The large peak around $m_X^2 = 0$ corresponds to $K_S K_S$ events, whereas the contribution near $m_X^2 \approx 0.02\ \mathrm{GeV}^2$ is due to contaminant $K_S K_S \pi^0$ events. The line shows a Monte Carlo simulation whose input intensity of $K_S K_S$ and $K_S K_S \pi^0$ events corresponds to a cross-section ratio consistent with previous experiments [16].

Figure 3. Total cross-section data for the reaction $\bar{p}p \to K_S K_S$ from this experiment. No resonance structure is observed. The reported mass and width of the ξ resonance from Ref. [1] are indicated. The dashed line shows a fit using the parameterisation of Eqn. (1).

Figure 4. Acceptance-corrected and normalised differential cross-section data for $\bar{p}p \to K_S K_S$ obtained when grouping together all energy settings of the scan. The dashed line shows a Legendre polynomial fit using Eqn. (3) with $k_{max} = 2$.

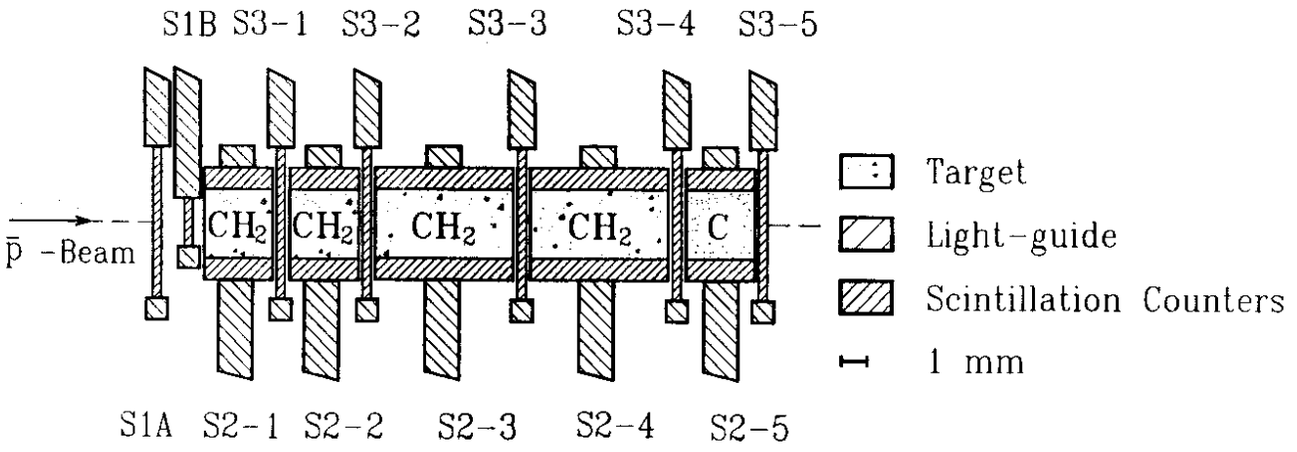
S1B S3-1 S3-2 S3-3 S3-4 S3-5
$\bar{p}$ -Beam
CH_2
CH_2
CH_2
CH_2
C
Target
Light-guide
Scintillation Counters
1 mm
S1A S2-1 S2-2 S2-3 S2-4 S2-5

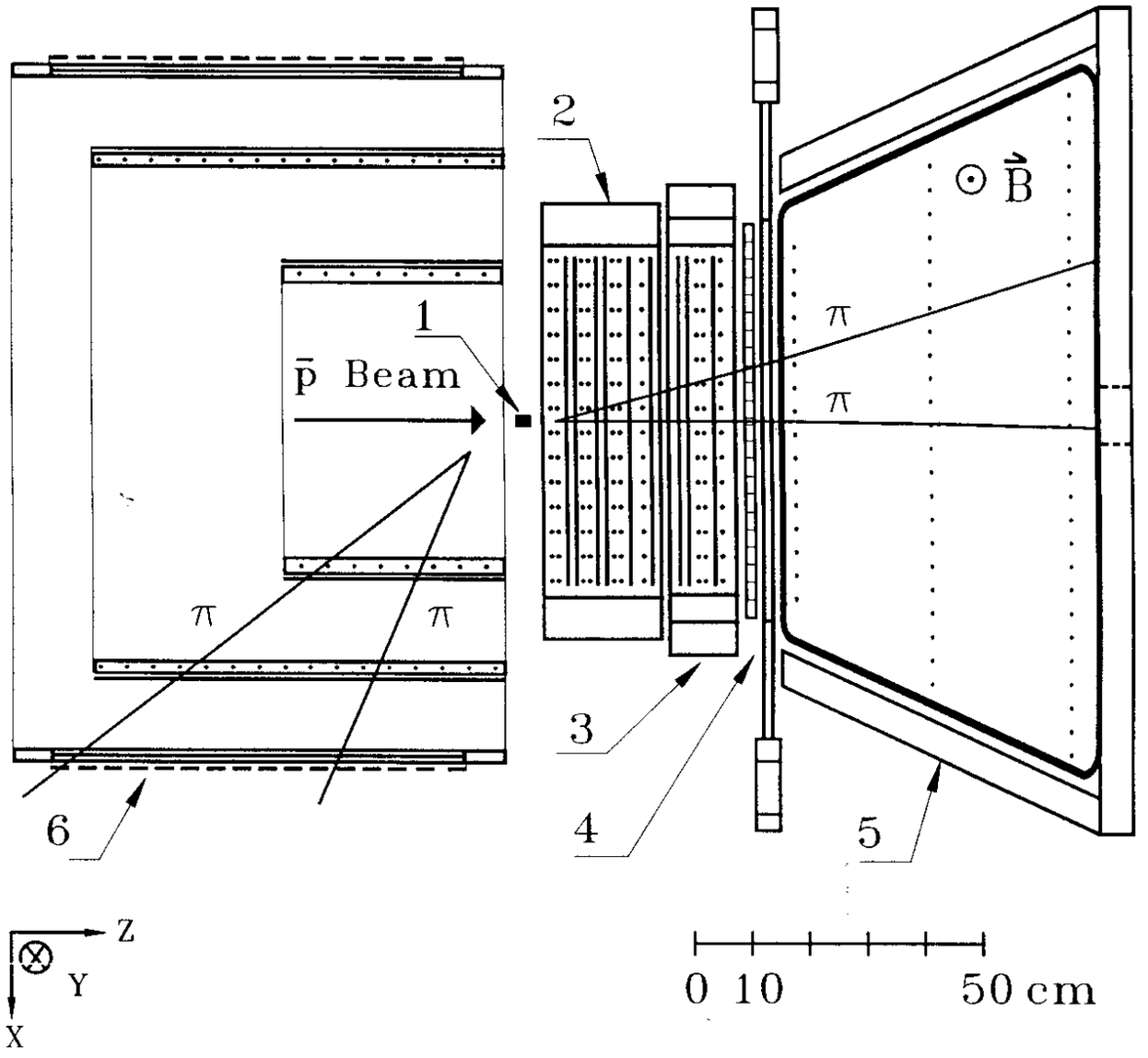
2
1
$\bar{p}$ Beam
$\odot \vec{B}$
π
π
π
π
3
4
5
6
Z
Y
X
0 10
50 cm

Figure 1.

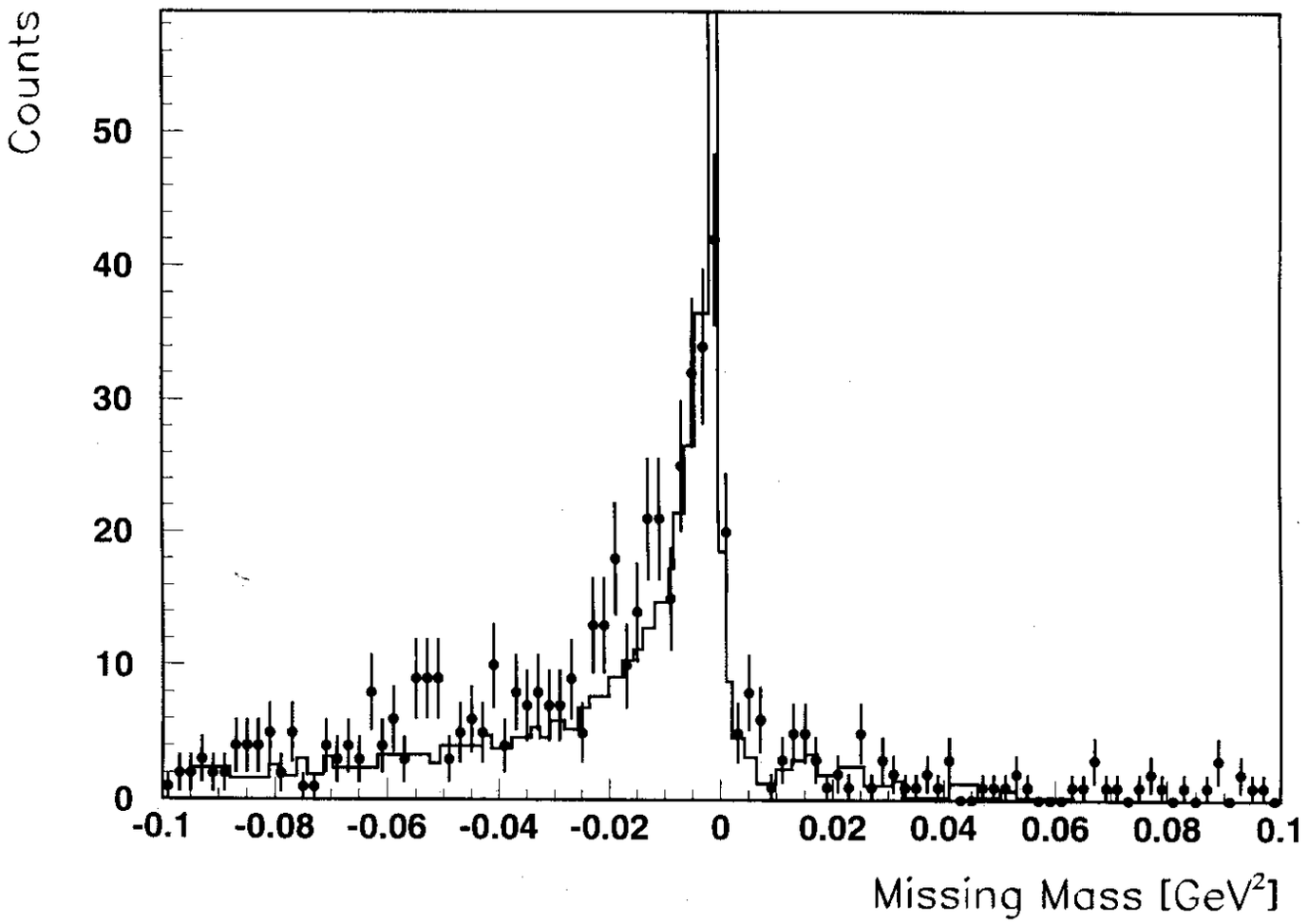
Counts
50
40
30
20
10
0
-0.1
-0.08
-0.06
-0.04
-0.02
0
0.02
0.04
0.06
0.08
0.1
Missing Mass [GeV²]

Figure 2.

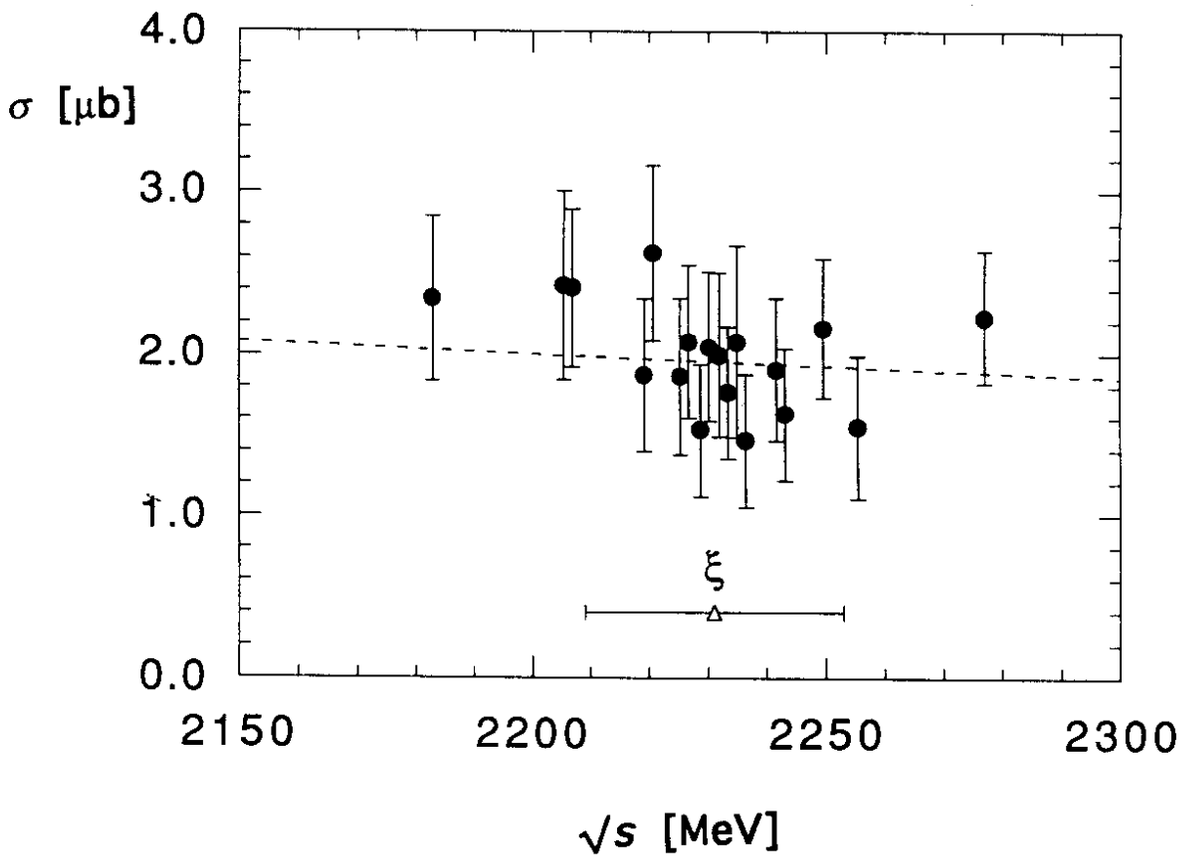

Figure 3.

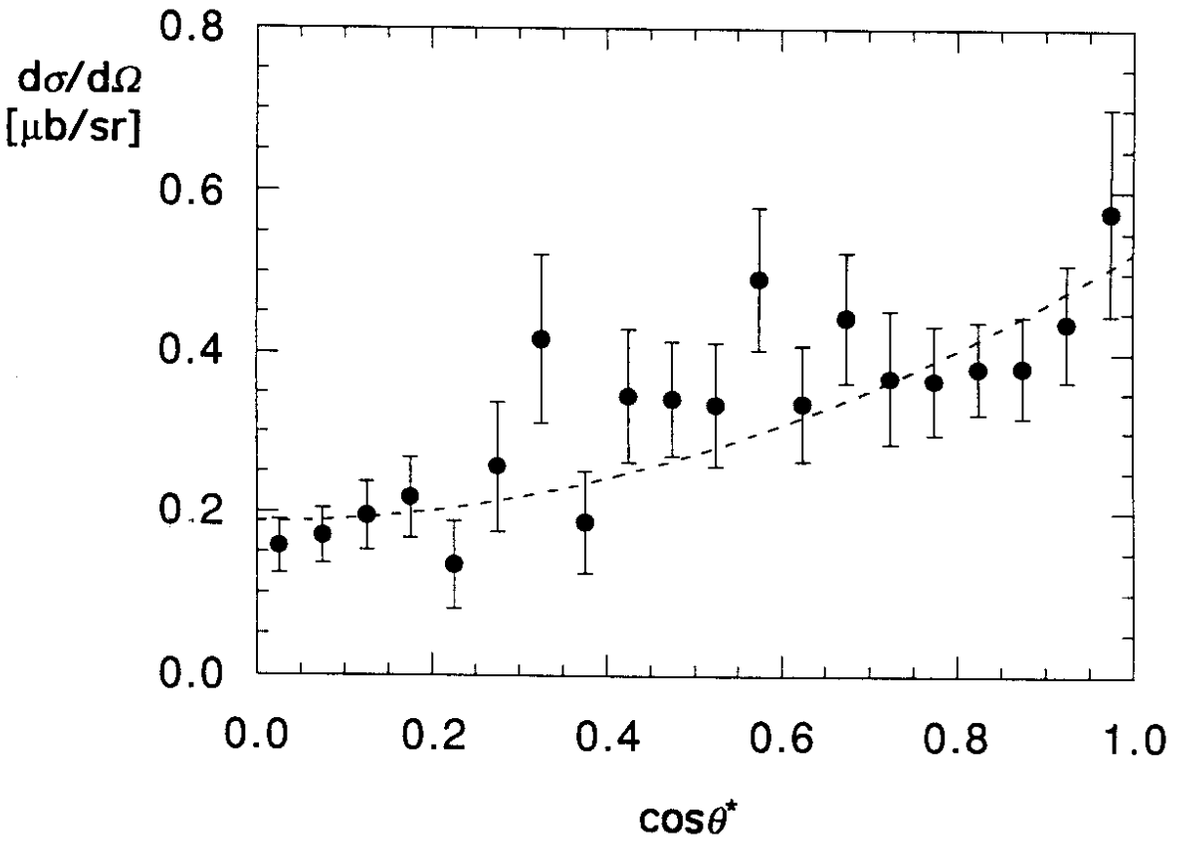

Figure 4.